

Theoretical prediction of the structural, electronic, thermodynamic and thermoelectric properties of Heusler alloys CrCoLaZ (Z=Ga, Si): New Candidate for Spintronics

kamel HOCINE

University of Relizane

Youcef GUERMIT

gyoucef75@gmail.com

University of Relizane

Research Article

Keywords: FP-LAPW, Heusler, electronic properties, thermodynamic properties, thermoelectric properties, half-metal

Posted Date: April 10th, 2024

DOI: <https://doi.org/10.21203/rs.3.rs-4193178/v1>

License:  This work is licensed under a Creative Commons Attribution 4.0 International License.

[Read Full License](#)

Additional Declarations: No competing interests reported.

Theoretical prediction of the structural, electronic, thermodynamic and thermoelectric properties of Heusler alloys CrCoLaZ (Z=Ga, Si): New Candidate for Spintronics.

Kamel HOCINE ^{1,2}, Youcef GUERMIT ^{1,2,*}

¹ Faculty of Science and Technology, University of Relizane, Bourmadia city, BP48000, Relizane, Algeria

² Magnetic Materials Laboratory (LMM), Djillali Liabes University of Sidi-Bel-Abbes, BP 89 Sidi Bel Abbes 22000-Algeria.

- gyoucef75@gmail.com

Abstract

An ab-initio calculation was performed using the linearized augmented plane wave method (FP-LAPW), within the framework of density functional theory (DFT), with the generalized gradient approximation GGA to calculate the structural, electronic, magnetic, thermodynamic and thermoelectric properties of quaternary Heusler CrCoLaZ alloys (Z=Ga, Si) which are of technological interest in the field of spintronics research. Calculations show that CrCoLaZ (Z=Ga, Si) compounds having characteristics of ferromagnetic half-metal with a gap of 0.6 eV. Using the quasi-harmonic Debye model, the variations of lattice parameter, thermal expansion coefficient, heat capacities and Debye temperature with pressures covering the 0–20 GPa interval and temperatures ranging from 0 to 1200 K were also investigated and in-depth discussed. The results of our simulation have been interpreted and compared to the theoretical results available. Furthermore, BoltzTrap package is used to compute thermoelectric parameters such as density of states, Seebeck coefficient S , electrical conductivity (σ/τ), electronic thermal conductivity (κ/τ) and the figure of merit (ZT). These parameters are computed at three different temperature ranges 300, 500 and 800 K to explore the potential of these compounds for high-performance technological applications.

Keywords: FP-LAPW; Heusler; electronic properties; thermodynamic properties; thermoelectric properties; half-metal..

*E-mail address: gyoucef75@gmail.com (Dr. Y. GUERMIT)

1. Introduction

Heusler alloys have attracted the attention of several scientific researchers due to their surprising properties. Half-metallic magnetism is one of these properties. [1-6], magnetic shape memory behavior [7-11], spin gapless semiconductor [12-15], giant magnetocaloric [16, 17], thermoelectric effects [18, 19], superconductivity [20]. These properties effectively impact several technological applications. For example, half-metals are used as spin injectors, magnetic tunnel junctions, spin valves, and spin torque transfer random access memories [21]. Heusler alloys are divided into two major families based on their chemical composition. The first family is known as Half-Heusler with general chemical formula XYZ, it crystallizes in structure $C1b$ with space group $F43m$, where X and Y represent transition metals and Z is sp element. The second family is the full Heusler and has stoichiometry X_2YZ , it crystallizes in structure $L21$ with space group $Fm-3m$ [22-24]. Another class of Heusler compounds of the $LiMgPdSn$ type is formed by the substitution of the X atom by an X' atom. This gives a quaternary compound of formula $(XX')YZ$, where X is a transition metal. The valence of X' is lower than that of X , and the valence of the element Y is lower than that of X and X' [25, 26]. Several studies on quaternary Heusler alloys can be found in the literature. As an example, we cite the $CrLaCoZ$ alloys ($Z = Al, Ga, In, Ge, Sn, Pb$) studied by Liu [27], who found that these compounds are half-metals obeying the Slater-Pauling rule. Priyanka and. Al [28] studied the electronic, mechanical and thermoelectric properties of the quaternary compounds $CoZrCrZ$ ($Z = Al, Ga, In$). In addition, Heusler $CoScCrZ$ ($Z = Al, Ga, Ge, In$) alloys were investigated for various physical properties by Shakil and. Al [29] and concluded that these compounds are possible candidates for applications in spintronics and thermoelectrics. Other studies interested in the theoretical calculation of the structural, electronic and elastic properties of the alloys $CoNbCrZ$ ($Z = Al, Ga, Si, Ge$) [30], $NbCoCrAl$ and $NbRhCrAl$ [31] using codes such as VASP and Korringa-Kohn -Rostoker (SPR-KKR). According to our extensive literature search, there are no experimental works or theoretical investigations available for the Heusler alloy $CrCoLaSi$. The aim of our work is to determine the structural, electronic, magnetic, thermodynamic and thermoelectric properties of quaternary Heusler alloys $CrCoLaZ$ ($Z=Ga; Si$) by the FP-LAPW method implemented in the Wien2K code under the GGA approximation [32].

II- Computational Details

The structural properties were determined using the Wien2K code [32], which is a direct application of the linear augmented plane wave method FP-LAPW [33, 34], by performing relativistic scalar calculations. For the determination of the exchange and correlation potential, we used the generalized gradient approximation GGA [35], for magnetic systems, we used the generalized

gradient approximation proposed by Perdew-Burke- Ernzerhof (GGA-PBE) [36]. We set the parameter $R_{mt} * K_{max}$, which controls the size of the bases, to 7. In these calculations, we used a default radius R_{mt} . The value of G_{max} is 12, where G_{max} is the norm of the largest wave vector used for the wave expansion of the charge density. The separation energy between the valence and core states is assumed -81.6 eV. The K integration on the Brillouin zone was performed with 3000 special points (14x14x14). In addition, we applied the quasi-harmonic Debye model implemented in the Gibbs pseudo code [37-40]. This allowed us to calculate the thermodynamic quantities at any temperature and pressure from the calculated E-V data at $T = 0$ K and $P = 0$ GP. To carry out these investigations, ab initio calculations using the FPLAPW method were performed to study the structural, magnetic, thermodynamic and thermoelectric properties of CrCoLaGa and CrCoLaSi.

III- RESULTS AND DISCUSSION

III- 1. Structural properties

In general, CrCoLaZ (Z=Ga; Si) quaternary alloys crystallize in three types of face-centered cubic (CFC) structures with space group F4-3m (216). The atomic positions of each type are given in Table 1 [41]. The representation of the crystal structure of CrCoLaZ compounds (Z=Ga; Si) for each type of structure is schematized in Figure 1:

Tableau 1: The three possible structures of Heusler CrCoLaZ quaternary alloys [41].

	Type I	Type II	Type III
Cr	(0 ; 0 ; 0)	(0.5 ; 0.5 ; 0.5)	(0 ; 0 ; 0)
Co	(0.25 ; 0.25 ; 0.25)	(0 ; 0 ; 0)	(0.5 ; 0.5 ; 0.5)
La	(0.5 ; 0.5 ; 0.5)	(0.25 ; 0.25 ; 0.25)	(0.25 ; 0.25 ; 0.25)
Z = G a, Si	(0.75 ; 0.75 ; 0.75)	(0.75 ; 0.75 ; 0.75)	(0.75 ; 0.75 ; 0.75)

In order to find the stable structure of the compounds CrCoLaGa and CrCoLaSi, we calculated the variation of the total energy as a function of the volume in the ferromagnetic state (FM) and in the non-magnetic state (NM) for each type of the previous structures.

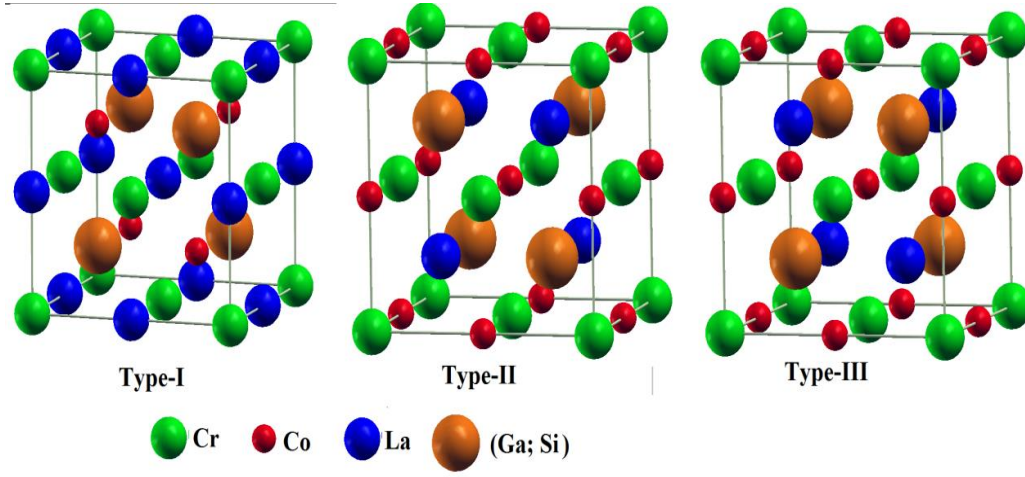


Figure 1: Crystal structures of the three types for CrCoLaZ (Z=Ga; Si).

The equilibrium parameters such as the lattice parameter (a_0), the compressibility modulus B_0 and its derivative B' were obtained by fitting the total energy E_{tot} (eV) as a function of the volume V (\AA^3) using the Murnaghan equation of state [42]:

$$E(V) = E_0 + \frac{B_0}{B'_0} \left[\frac{\left(\frac{V_0}{V}\right)^{B'_0}}{B'_0 - 1} + 1 \right] - \frac{B_0 V_0}{B'_0 - 1} \quad (1)$$

Where, B_0 and B' are bulk modulus and pressure derivative of the bulk modulus in the equilibrium volume V_0 , respectively.

The graphical representation of the variation of total energy E_{tot} (eV) versus volume V (\AA^3) for CrCoLaGa and CrCoLaSi compounds is shown in Figures 2 and 3, respectively. From these figures, it can be seen that both compounds are mechanically stable in the ferromagnetic phase – type III. The values obtained for the lattice parameter a_0 , the compressibility modulus B_0 , its first derivative as well as the total energy E_0 calculated by the GGA approximation of the CrCoLaGa and CrCoLaSi compounds are shown in Table 2.

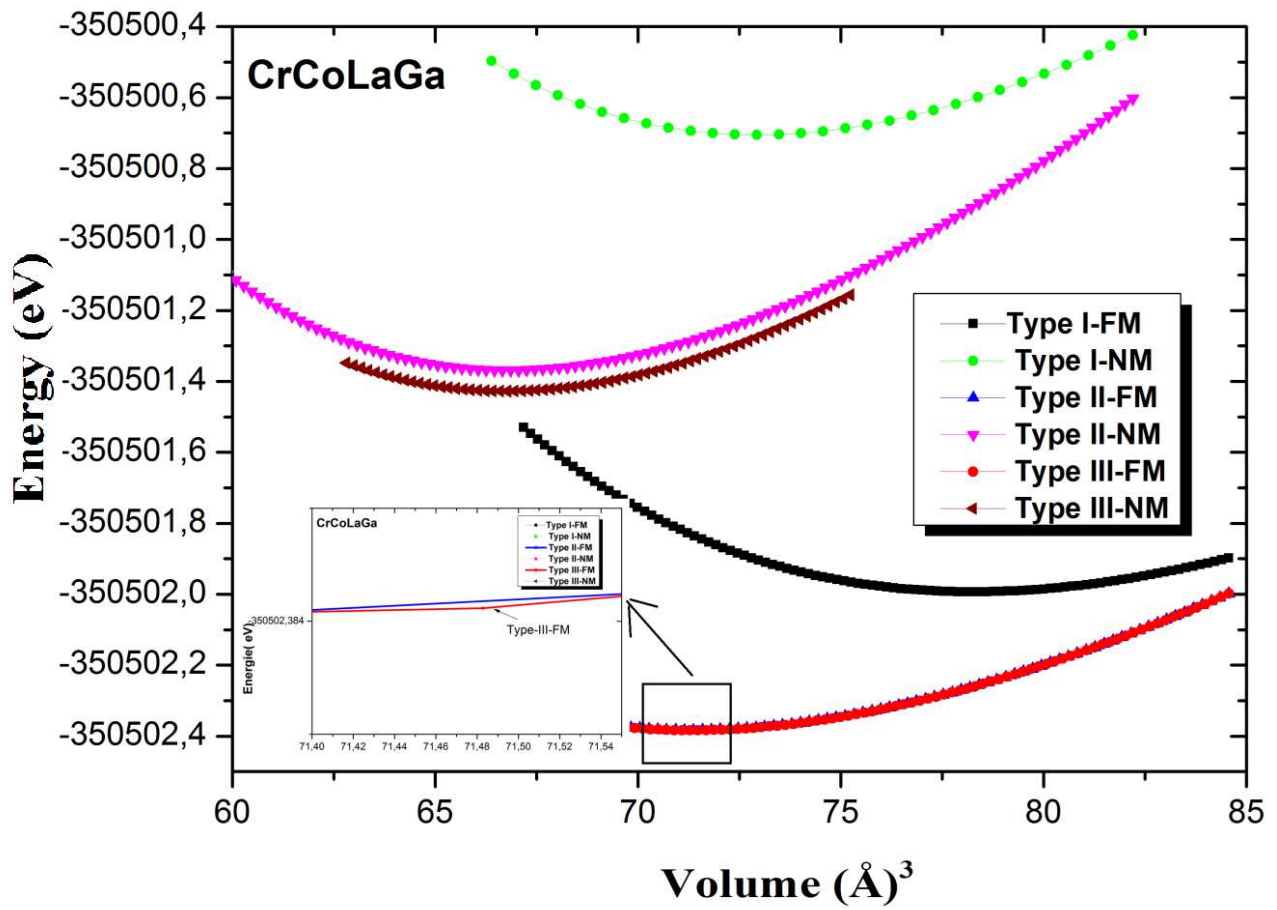


Figure 2: Variation of the total energy E_{tot} versus the unit cell volume for CrCoLaGa.

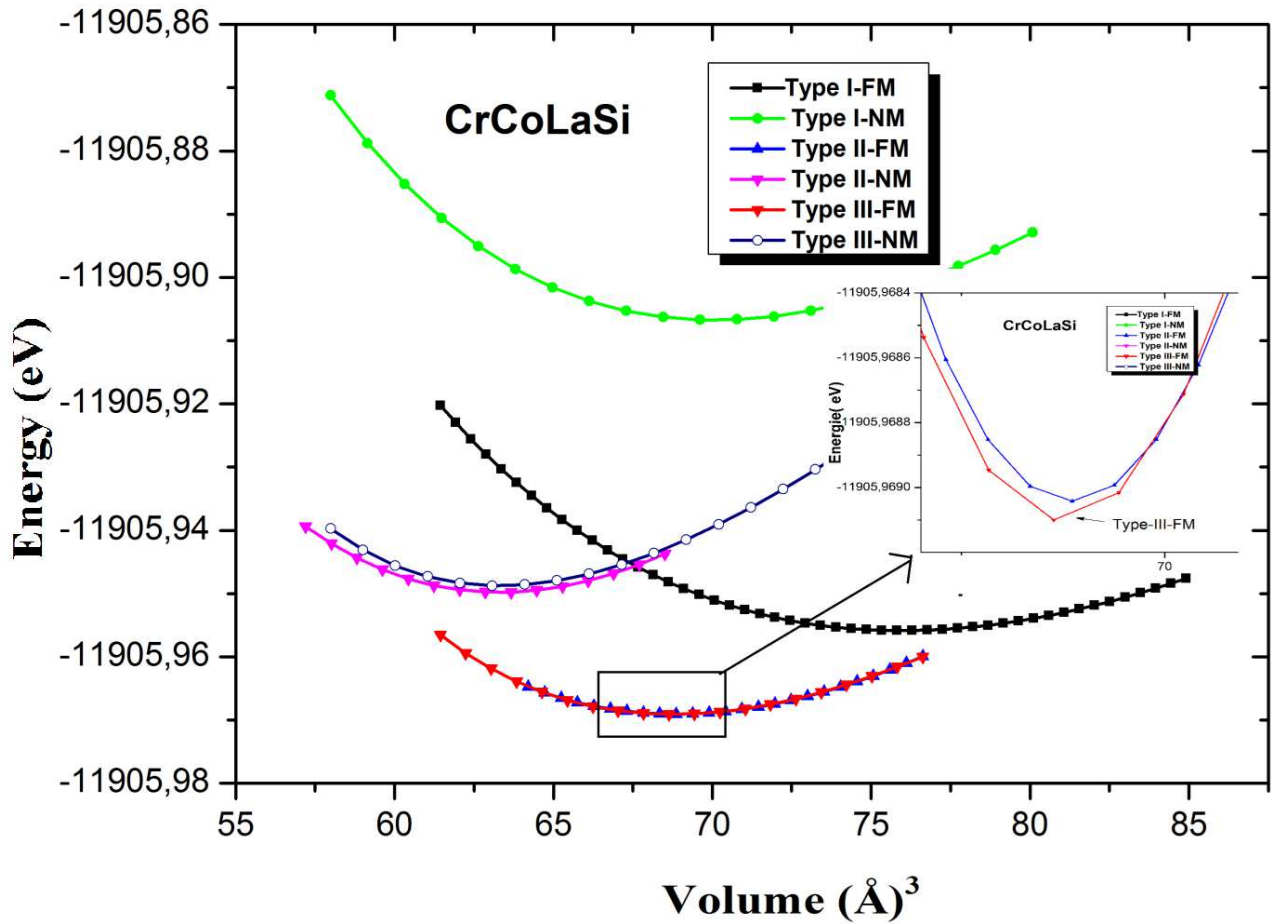


Figure 3: Variation of the total energy E_{tot} versus the unit cell volume for CrCoLaSi.

According to our bibliographic research, we did not find enough results to make a comparison with our calculations, except for the CrCoLaGa material in reference [43]. We found that the value of the lattice parameter of this compound in this reference is in good agreement with our result.

III-2. Electronic and magnetic properties

In this section we have used the ground state lattice parameters a_0 (Type III -FM) to calculate the electronic band structure (EBS) of the quaternary Heusler alloys CrCoLaGa and CrCoLaSi. Figures 4 and 5 visualize the BS for the spin up (majority spin) and spin down (minority spin) of the two compounds.

Tableau 2. Values of equilibrium lattice constant (a_0), bulk modulus (B), the pressure derivate of bulk modulus (B') and energy total (E_0) of the CrCoLaGa and CrCoLaSi.

compound	types	phase	$a(\text{\AA})$	$V_0 (\text{\AA}^3)$	B(GPa)	B'	$E_0 (\text{eV})$
CrCoLaGa	TypeI	FM	6.77	78,126	70.06	5.05	-350501,99389
		NM	6.61	72,920	90.79	4.07	-350500,70658
	TypeII	FM	6.57	71,283	70.62	5.02	-350502,38394
		NM	6.42	66,807	90.47	4.37	-350501,36912
	TypeIII	FM	6.57	71,303	78.64	5.01	-350502,44244
		NM	6.42	66,744	99.749	4.45	-350501,42712
			6.582[43]				
CrCoLaSi	TypeI	FM	6.71	75,979	76.47	3.45	-305511,3203
		NM	6.53	70,074	100.37	4.17	-305510,0599
	TypeII	FM	6.49	68,942	101.28	3.57	-305511,65845
		NM	6.31	63,296	135.20	6.15	-305511,1379
	TypeIII	FM	6.49	68,739	104.39	5.47	-305511,6599
		NM	6.31	63,304	128.79	2.75	-305511,1648

The analysis of these figures shows that the quaternary Heusler compounds CrCoLaGa and CrCoLaSi exhibit a half-metallic behavior. Indeed, for the majority spins we observe an overlapping of the bands at the Fermi level with zero energy gaps, unlike for the minority spins. For the latter, we observe the existence of an indirect gap with a value of 0.56 eV for CrCoLaGa and 0.62 eV for CrCoLaSi,

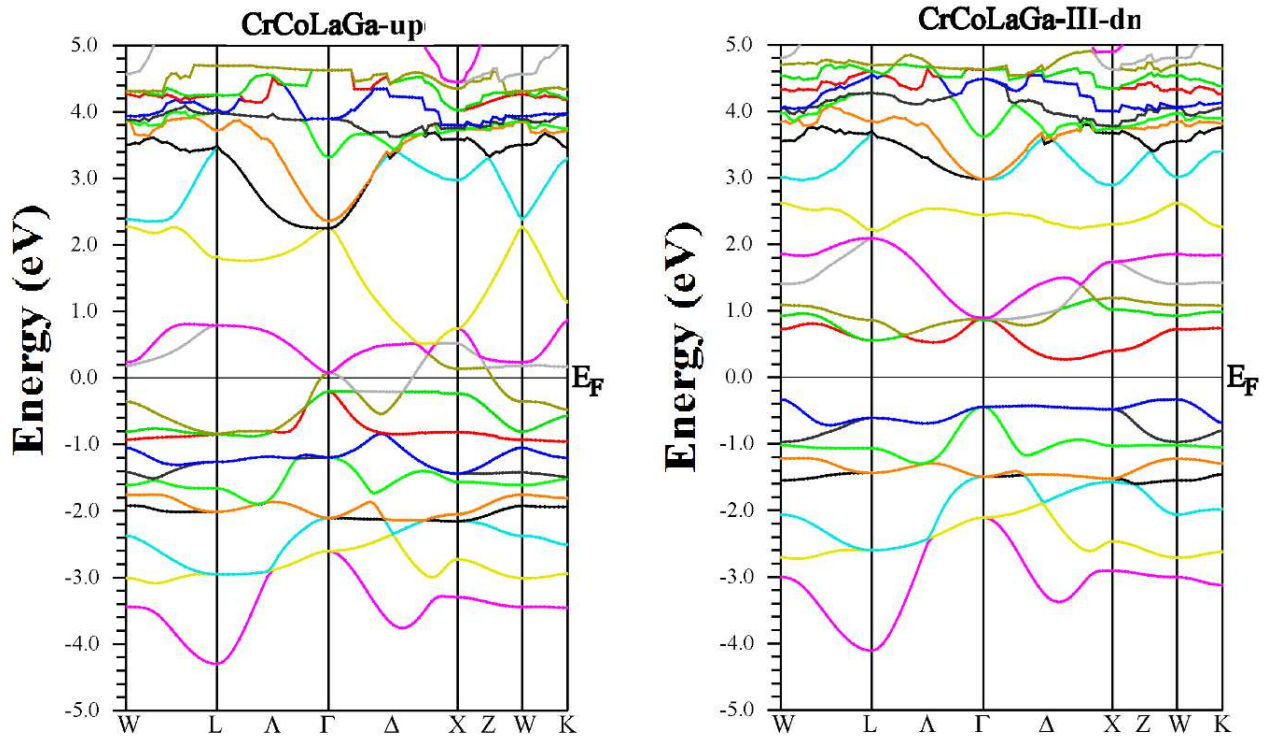


Figure 4: The band structure for the majority-spin (left) and the minority-spin (right) of

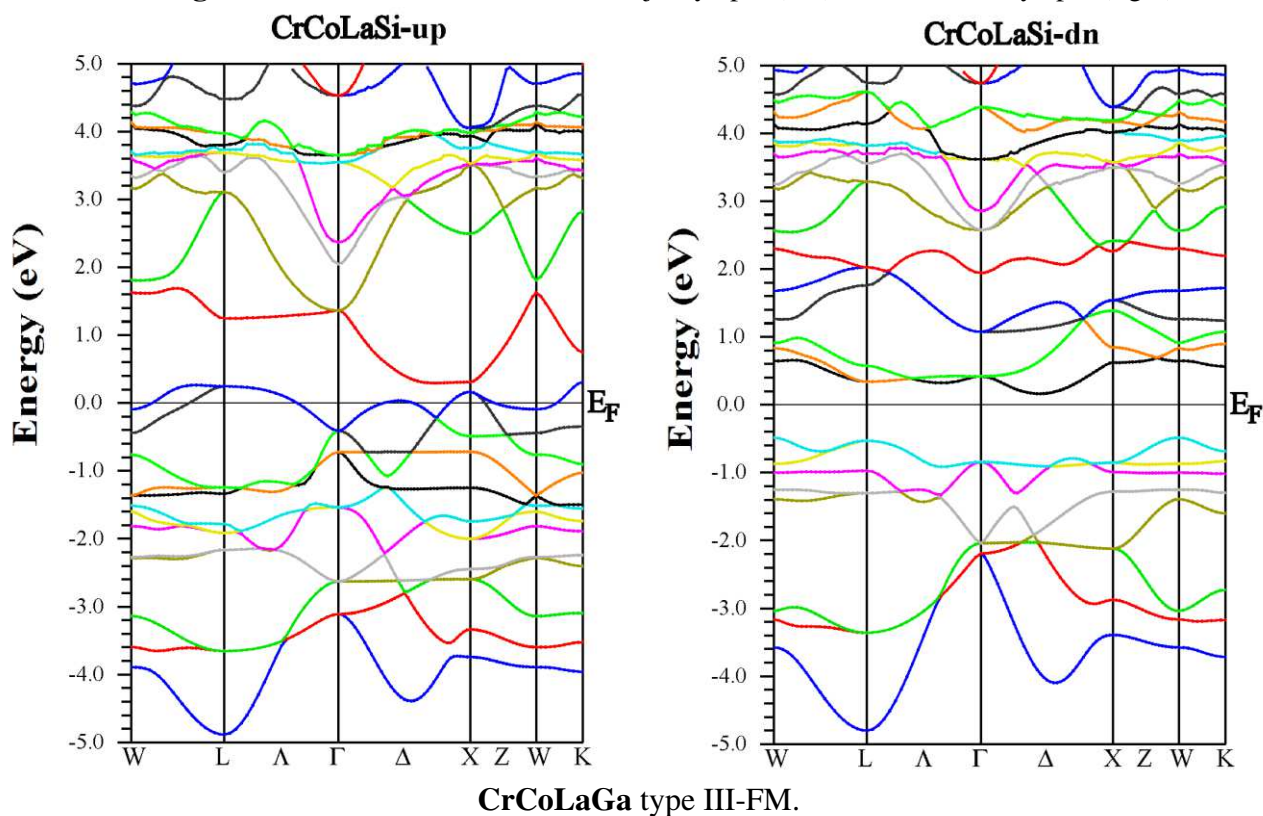


Figure 5: The band structure for the majority-spin (left) and the minority-spin (right) of **CrCoLaSi** type III-FM

Figs. 6 and 7, show the calculated spin-dependent total density of states (TDOS) and atom resolved partial density of states (PDOS) for the two quaternary Heusler compounds CrCoLaZ (Z= Ga,Si) with the FM type (III) structure at equilibrium lattice constants. It is obvious from the TDOS of these Heusler alloys, the majority spin version are metallic in nature while the minority spin version have a semiconducting character. According to the examination of PDOS for both compounds, we see that there is a strong presence of s-Ga and s-Si states in the energy interval [-10,-5 eV]. In the energetic region [-5,-2.5 eV], there is a strong contribution between p-Ga and Cr-deg(up) states (fig.6), while in fig 7 and in the same region, there is a strong hybridization between the p-Si, d-Cr and d-Co states. In the energy interval [-2.5,-1eV] (Fig. 6), there is a strong presence of d-t_{2g}-Co (down), d-Cr (up) states and a small population of p-Ga states. From fig .7 and in the same interval, a strong presence of d-Co states (up and down) and d-Cr states (up). Around the Fermi level, it is constituted only by the states d-Cr (up) and d-Co (up) for both compounds and p-Si (up) for CrCoLaSi and p-Ga (up) for CrCoLaGa. In the conduction band, from 1 to 2.5 eV, strong presence of the d-eg (down) and d-t_{2g} (down) states for Cr and Co atoms for both alloys, while from 2.5 to 5 eV, we see a strong contribution of states d-La.

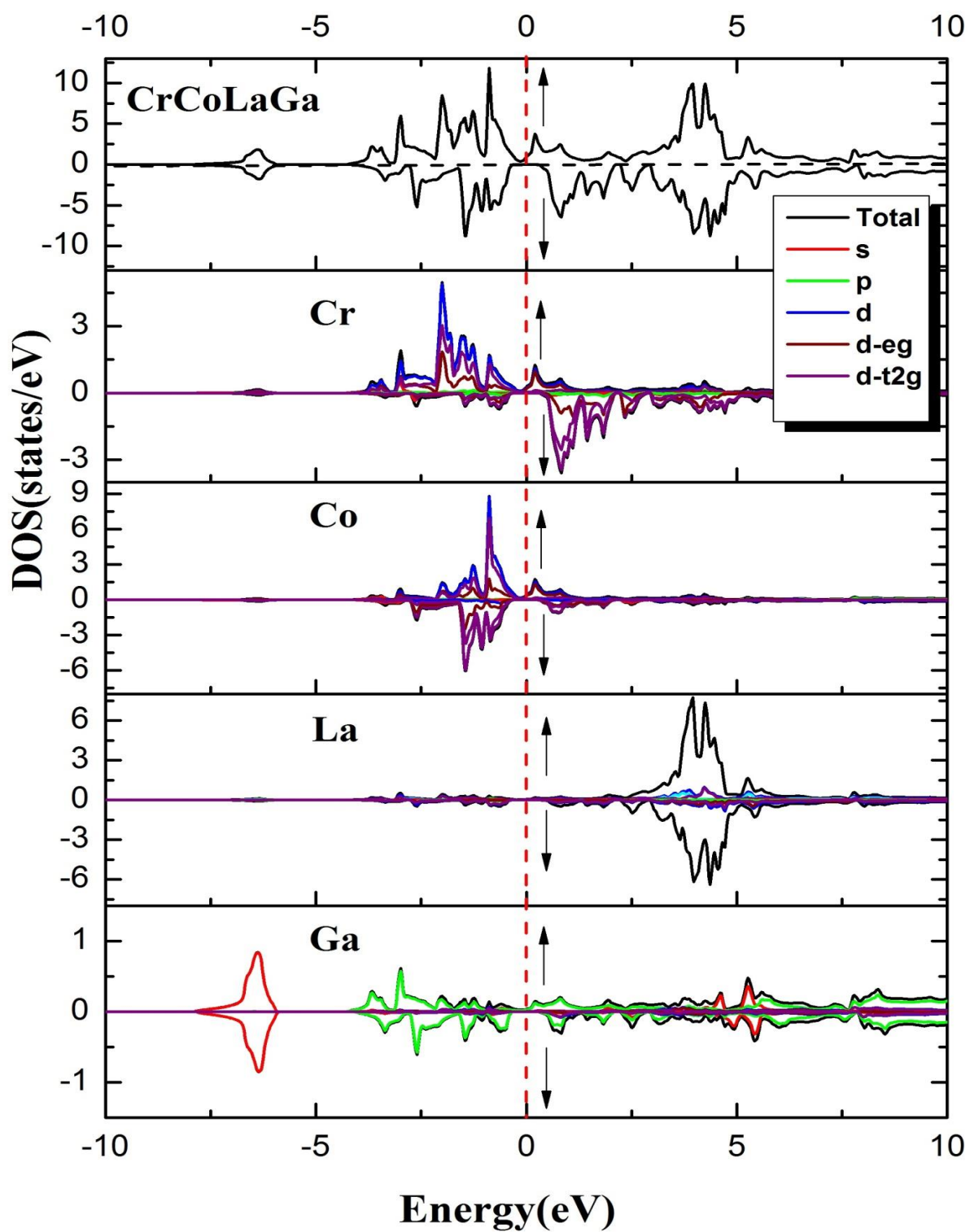


Figure 6: Total and partial spin-polarized density of states for CrCoLaGa.

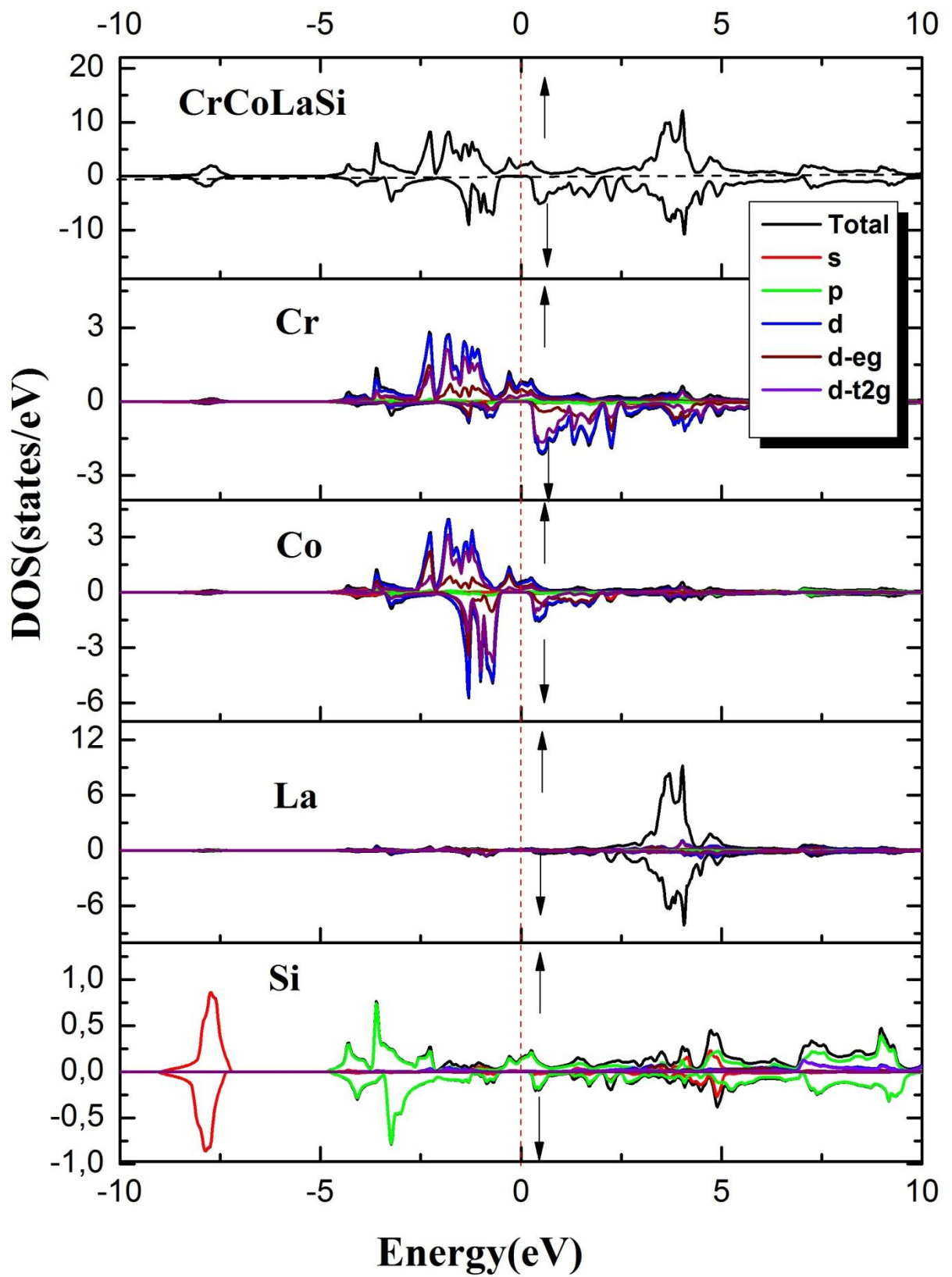


Figure 7: Total and partial spin-polarized density of states for CrCoLaSi.

Magnetic properties tell us in particular about the magnetic moment of a material, which is a very important indicator of the speed of the magnetic field in one material compared to another. Table 3 summarizes the values obtained for the total and atom-resolved spin magnetic moments at equilibrium for the Heusler compounds CrCoLaGa and CrCoLaSi. As shown in Table 3, the total magnetic moment (MM_{tot}) for the CrCoLaGa compound ($3.210 \mu_B$) is quite comparable to the result of the previous theoretical study [44]. In addition, we note that the MM_{tot} of the CrCoLaSi compound ($3.16 \mu_B$) is higher than the MM_{tot} of the CrCoLaGa compound. This increase is mainly due to the high contribution of the magnetic moment of the chromium atom.

Tableau 3: Total, atom-resolved, and interstitial spin magnetic moments for CrCoLaGa and CrCoLaSi.

Structure		Magnetic Moment in μ_B						
		Cr	Co	La	Ga	Si	Intersti-tial	MM_{tot}
CrCoLaGa	Present work	3.210	-0.267	0.015	-0.073		0.095	2.98
	Theoretical [43]	3.69	- 0.10	- 0.35	- 0.24			3.00
CrCoLaSi	Present work	3.16	0.84	-0.056		-0.12	-0.108	3.72

The contribution of the magnetic moments of the atoms of Silicium and Gallium in MM_{tot} for the two compounds is low and its atom –resolved spin magnetic moments have negative values.

III-3. Chemical bonds

The bonding character of materials is determined by the distribution of electrons in the charge density contour plots. The nature of the bond (ionic or covalent) is related to the transfer of charge between the cation and anion of the atoms. In a polar (ionic) bond, the cation and anion pair is formed by the transfer of charge between the atoms, while a non-polar (covalent) bond is formed by the sharing of charge between the cation and anion. The charge density contour plots of the Heusler quaternary compounds CrCoLaGa and CrCoLaSi in the (001) crystallographic planes are shown in Figures 8 and 10, respectively. While the charge density contour plots of the two compounds in (011) planes are shown in Figures 9 and 11. From these figures we can conclude that there are two types of chemical bonds in the Heusler alloys CrCoLaGa and CrCoLaSi. The first bond, which is

the ionic bond, appears between the Cr atoms, where we notice a barrier between them, and this is due to a difference in the ability to lose or gain electrons. The second bond, which is the covalent bond that results from the contribution of Cr and Co atoms by an electron from its valence level.

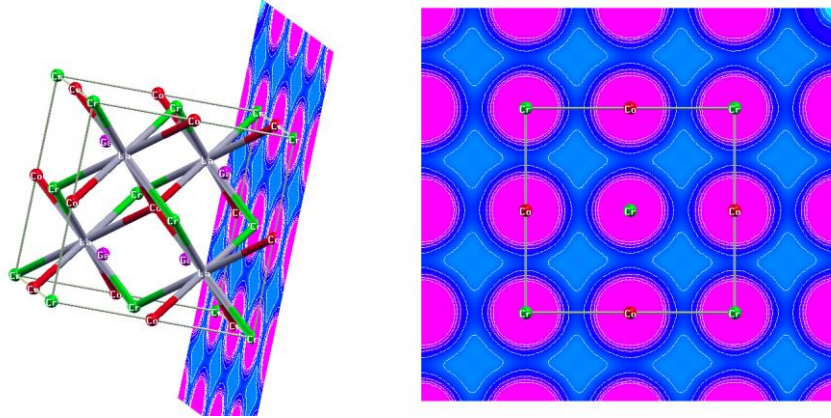


Figure 8: The charge density contours plot of CrCoLaGa in (001) plane.

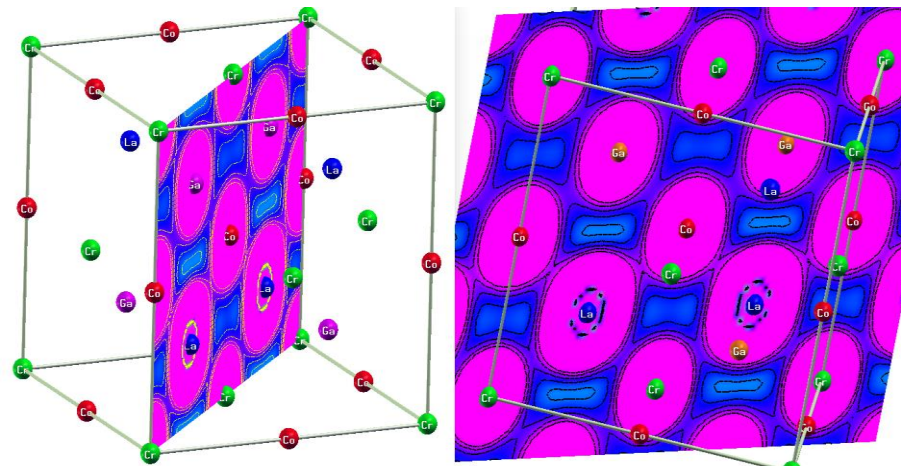


Figure 9: The charge density contours plot of CrCoLaGa in (011) plane

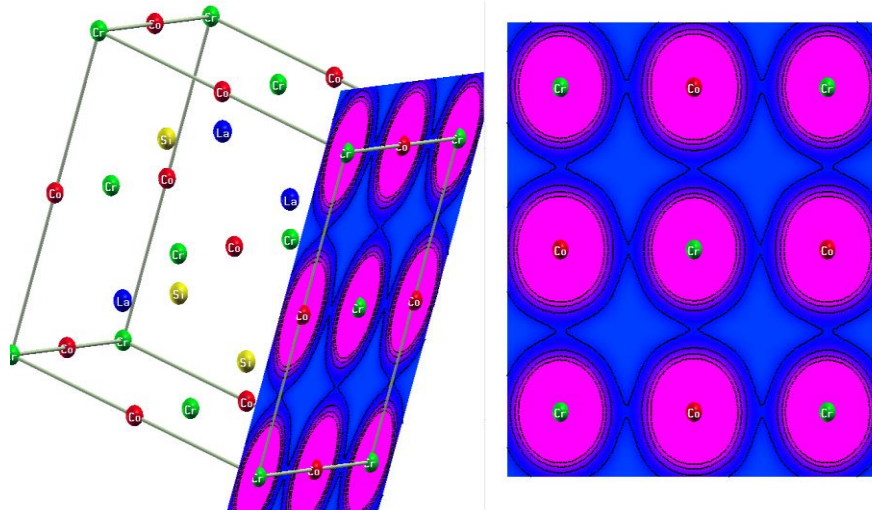


Figure 10: The charge density contours plot of CrCoLaSi in (001) plane

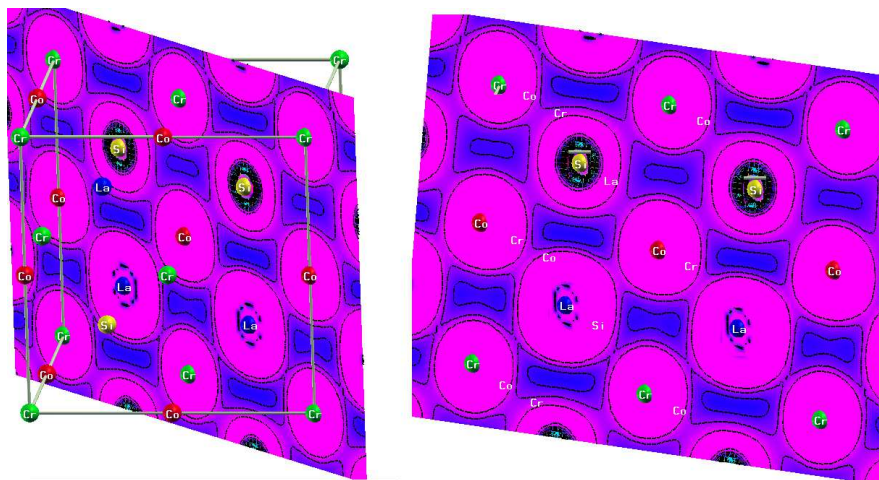


Figure 11: The charge density contours plot of CrCoLaSi in (011)

III-4. Thermodynamic properties

According to the laws of dynamics, when the lattice temperature is above absolute zero, its energy is not constant, but fluctuates randomly around the mean value. These energy fluctuations are due to random vibrations of the lattice, which can be seen as a gas of phonons, and since these phonons are related to the lattice temperature, they are sometimes called thermal. Phonons are concepts of quantum mechanics, and their study occupies an important place in condensed matter physics. They play an important role in many properties of solids, including heat capacity, thermal conductivity, and electrical conductivity. The behavior of phonons is studied by Debye's quasi-harmonic model, which is an explanation of the behavior of the heat capacity of solids as a function of temperature, developed by Peter Debye in 1912 [44]. It consists in studying the vibrations of the network of atoms that make up the solid. This model makes it possible to explain precisely the experimental values; it also agrees with the law of Dulong and Petit [45] at high temperature. In this section, we

have used the Debye quasi-harmonic model to calculate the thermodynamic properties such as the variation of volume, the specific heat capacity at constant volume (C_V), specific capacity (C_P), the Debye temperature and the coefficient of thermal expansion as a function of temperature of CrCoLaGa and CrCoLaSi. The thermal properties are determined in the temperature range from 0K to 1200 K, where the quasi-harmonic model remains fully valid. The pressure effect has been studied in the range of 0 to 20 GPa.

The variation of volume with respect to temperature at different pressures is shown in Fig. 12. It was found that the volume increases slightly with increasing temperature.

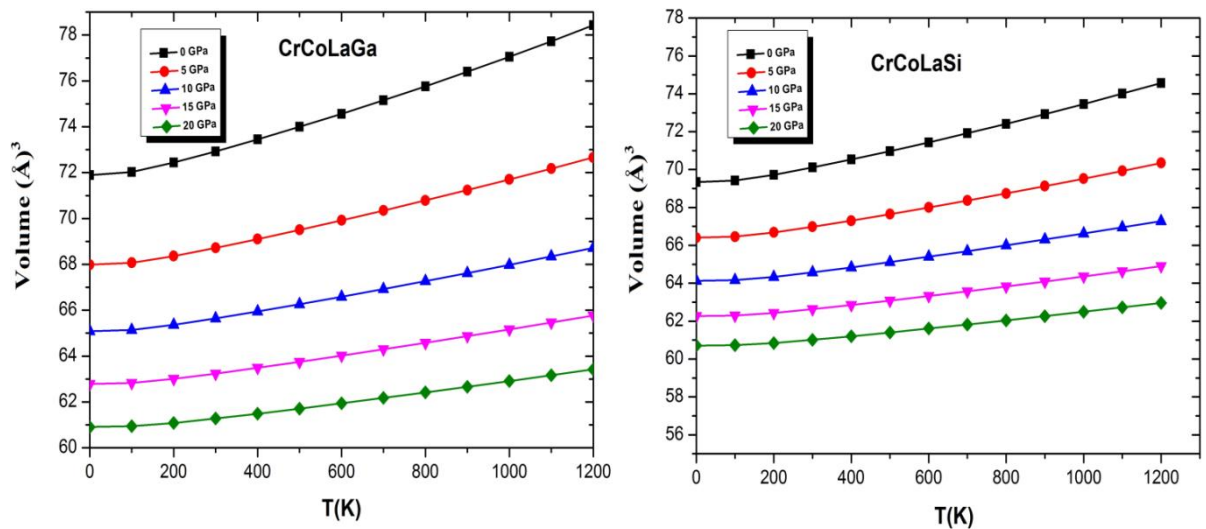


Figure 12: The temperature effects on the lattice parameter for CrCoLaGa and CrCoLaSi alloys.

The investigation of C_V as a function of the temperature at different pressures of 0, 5, 10, 15 and 20 GPa is shown in Fig 13. At high temperatures, C_V tends to the Dulong and Petit limit, which is rather common for all solids. At sufficiently low temperatures, C_V is proportional to T^3 . While at 300K and 0 GPa, the heat capacity for the CrCoLaGa and CrCoLaSi compounds are found to be 97.05 J mol⁻¹ K⁻¹ and 93.12 J mol⁻¹ K⁻¹, respectively. Figure 14 illustrates how the temperature (T) at different pressures affects the CrCoLaGa and CrCoLaSi alloy's specific capacity (C_P) under constant pressure. It is found that the specific capacity increases quickly when $T \geq 200$ K and that C_P becomes stable and trends toward infinity when $T \geq 500$ K. Figure 15 represent the variation of the Debye temperature as a function of temperature. We notice that the Debye temperature is inversely proportional to the temperature. As the temperature increases, the Debye temperature continuously decreases. The Debye temperatures of the Heusler alloys CrCoLaGa and CrCoLaSi at 300K and 0 GPa pressure are 300 K and 375 K, respectively. This indicates that the compound CrCoLaSi is harder than CrCoLaGa compound. Figure 16 represents the variation of the thermal

expansion coefficient α (T) of CrCoLaGa and CrCoLaSi as a function of the temperature and the pressure. It is shown that, at a constant pressure and at low temperatures, α increases with temperature—especially at zero pressure—and gradually tends to a linear increase at higher temperatures. As the pressure increases, the increase of α with the temperature becomes smaller, while at a constant temperature, α decreases strongly with increasing pressure.

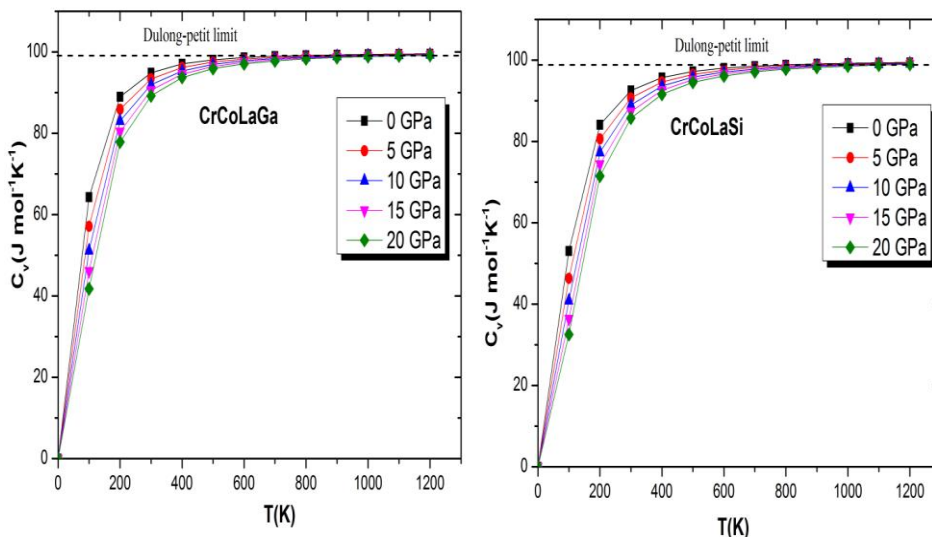


Figure 13: The heat capacity depending on the temperature for different pressures from 0 to 20 GPa for CrCoLaGa and CrCoLaSi alloys.

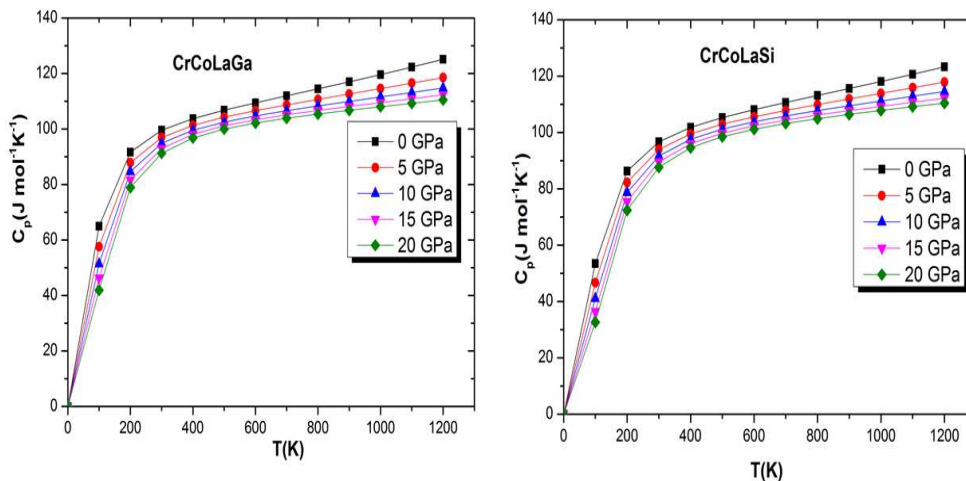


Figure 14: The specific capacity (C_p) depending on the temperature for different pressures from 0 GPa to 20 GPa for CrCoLaGa and CrCoLaSi alloys.

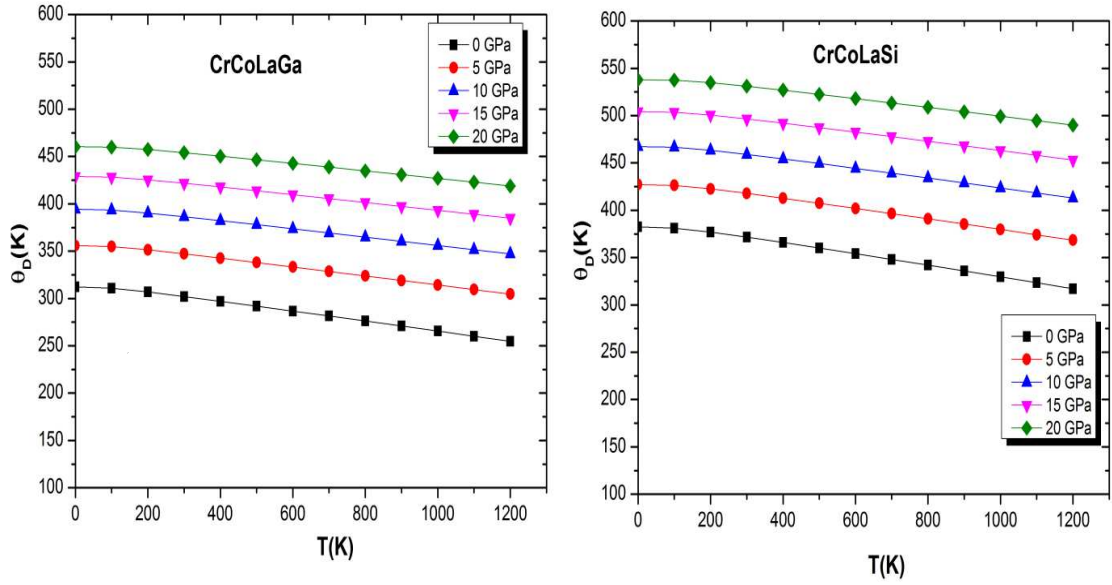


Figure 15: Variation of the Debye temperature with respect to the temperature at different pressures ranging from 0 to 20 GPa for CrCoLaGa and CrCoLaSi alloys.

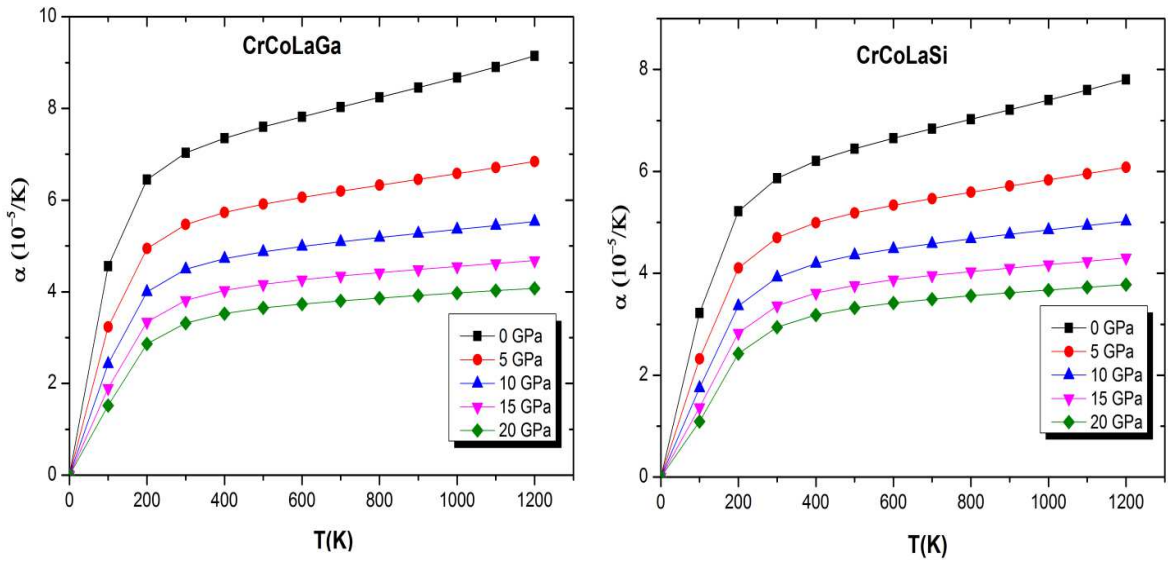


Figure 16: The thermal expansion coefficient as a function of the temperature at different pressures ranging from 0 GPa to 20 GPa for CrCoLaGa and CrCoLaSi alloys.

3.5 Thermoelectric properties

We used BoltzTrap package [46] to compute thermoelectric parameters. The method is based on Fourier expansion of band energies where space-group symmetry has been preserved by star functions. This method allows for the calculation of band structure-related quantities such as thermal and electrochemical properties. These properties allow for the assessment of transport parameters such as Seebeck coefficient, electrical conductivity, thermal conductivity and figure of merit (ZT) as a temperature (T) function. The latter parameter characterizes the performance of the material and the criterion of $ZT \geq 1$ is usually maintained for applications [47] and it is given by the relation:

$$ZT = TS^2 \frac{\sigma}{\kappa} \quad (2),$$

where S is the Seebeck coefficient, σ is the electrical conductivity, κ is the thermal conductivity, and T is the absolute temperature. Good thermoelectric materials have a high figure of merit, Seebeck coefficient and electrical conductivity, low thermal conductivity and power factor PF defined as:

$$PF = S^2 \sigma$$

For both spin channels, these parameters have been analyzed at three different temperature ranges 300, 500 and 800 K, as shown in Figures 17 and 20. The values of S , σ/τ , κ_e/τ , PF and ZT at 300 K are summarized in Table. 4. We note that at 300 K, both compounds have large S in n-type carriers, with S decreasing with increasing temperature, and CrCoLaGa having larger S in both spin channels than CrCoLaSi. This is due to the different valence electrons of both compounds, resulting in an inverse relationship between n and S . The investigation of the electrical conductivity (σ/τ) as a function of $(\mu - \mu_0)$ shows that for all the cases the temperature 300 K induce the highest electrical conductivity in the p -type doping range, depicting at higher temperature the mobility increases by reducing the electrical conductivity. Generally, the thermal conductivity κ is expressed as $\kappa = \kappa_e + \kappa_L$ where κ_e is the electronic thermal conductivity and κ_L is the lattice thermal conductivity (the phonon vibrations). In the BoltzTrap code, the phonon energy is small so that the phonon–phonon and the electron–phonon interactions can be neglected in the calculation. The parameter (κ/τ) inversely affects the thermoelectric performance of the materials. Figures 17 to 20 show that the electronic conductivity increases with temperature in both compounds in the negative and positive regions of the chemical potential, with the maximum located in the p -type region, 17.99 and 29.93 at 800 K for CrCoLaGa and CrCoLaS, respectively. Finally, the power factor PF is an important quantity in the study of the efficiency of thermoelectric materials; it depends to ZT of Merit. From the PF analysis, we can see that the PF s of both compounds increase with increasing temperature. The variation of ZT with temperature reaches a maximum value of 0.97 at 300 K for both compounds; these values are due to the high Seebeck coefficient. The DOS as a function of temperature shows that semi-metallic behavior is preserved up to 800 K. All these observations indicate that the investigated compounds are half-metallic ferromagnetic (HMFs) and this behavior is preserved at high temperature. Therefore, Primer research of Jiangang He [47], Oded Rabina [48] and Tsunehiro Takeuchi [49], the present compounds are potential candidates for spintronic thermoelectric devices.

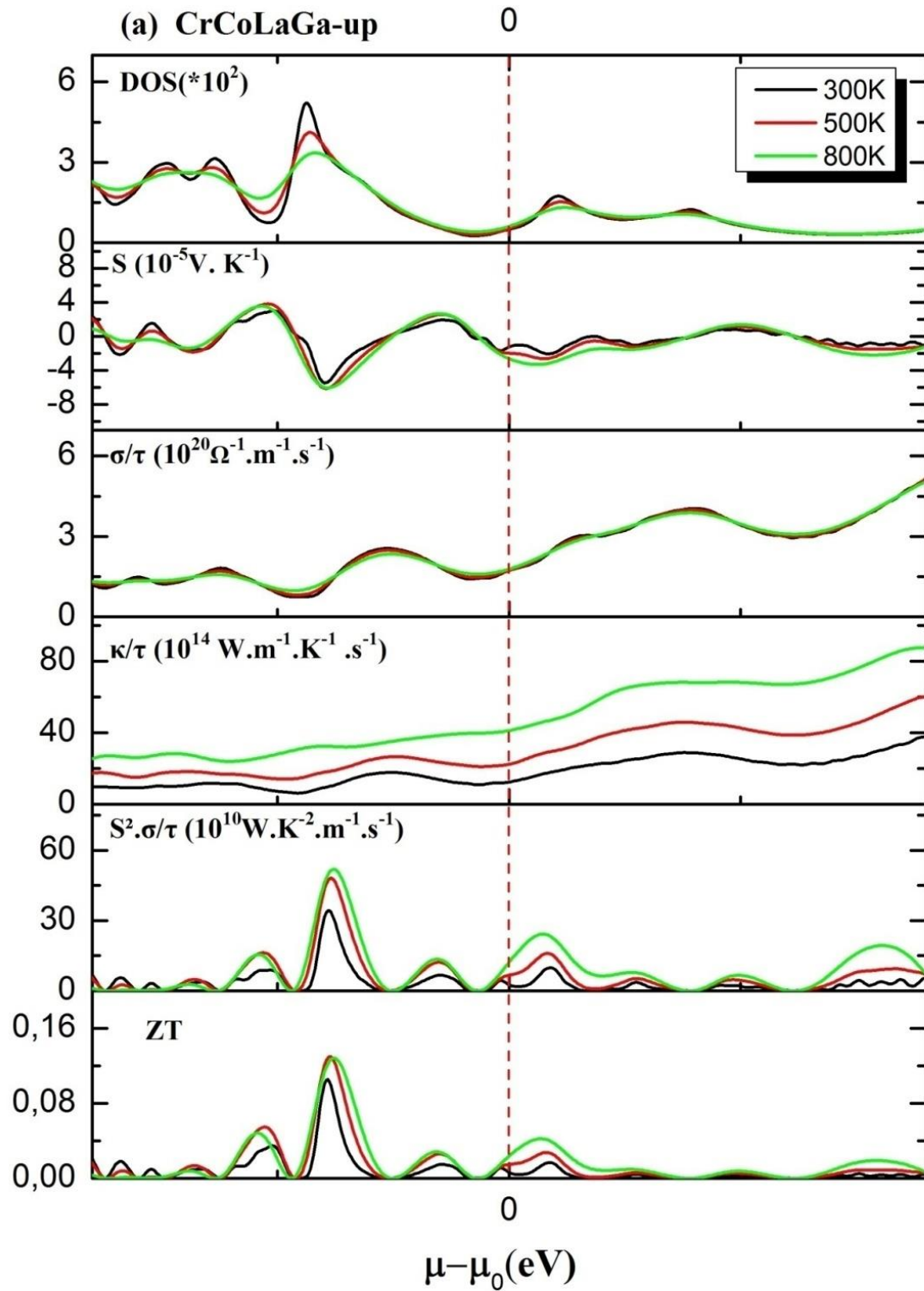


Figure17. Density of states, Seebeck coefficient S , electrical conductivity (σ/τ), electronic thermal conductivity (κ/τ), PF and the figure of merit (ZT) for CrCoLaGa-up Heusler compound

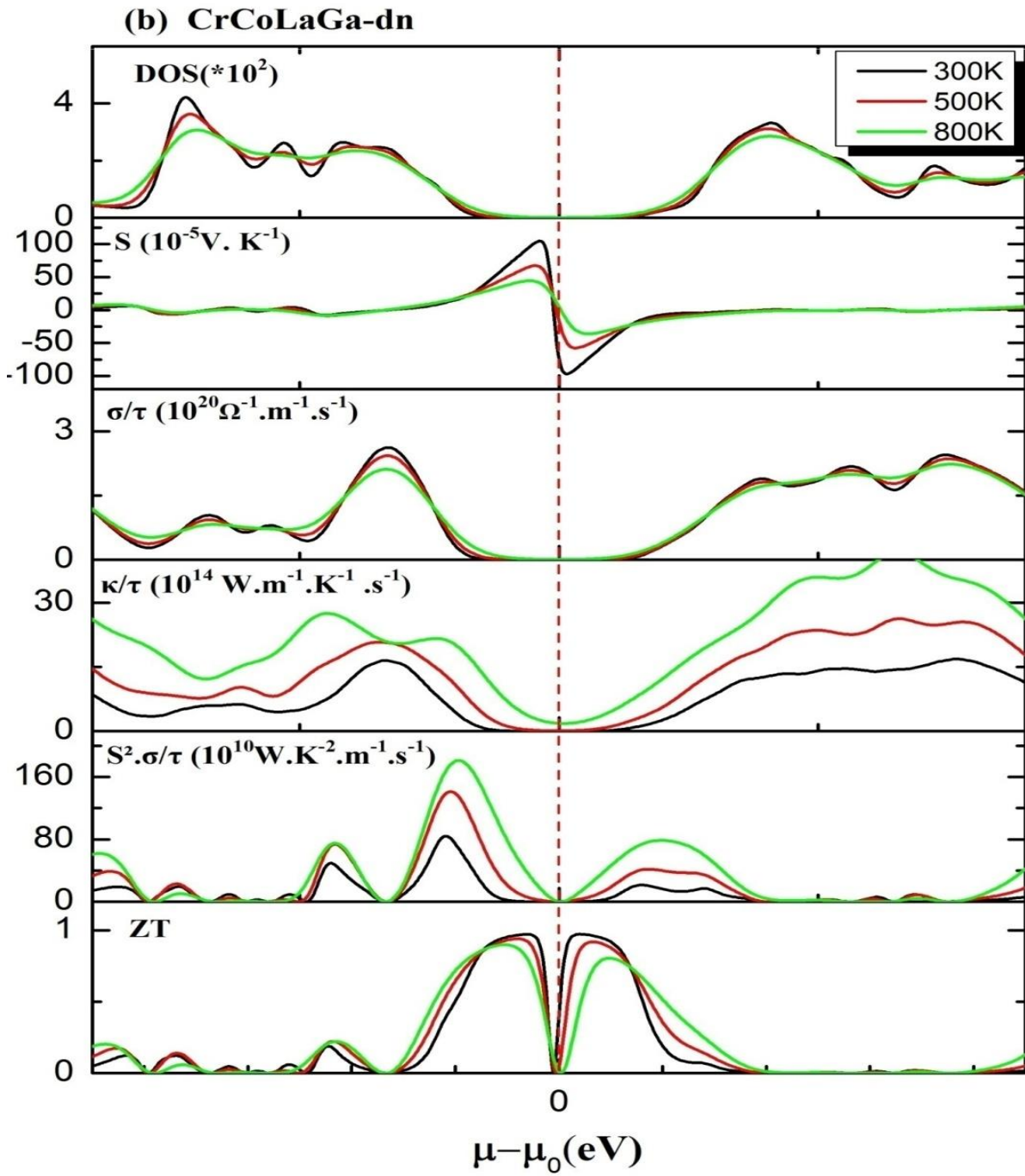


Figure18. Density of states, Seebeck coefficient S , electrical conductivity (σ/τ), electronic thermal conductivity (κ/τ), PF and the figure of merit (ZT) for CrCoLaGa-dn Heusler compound.

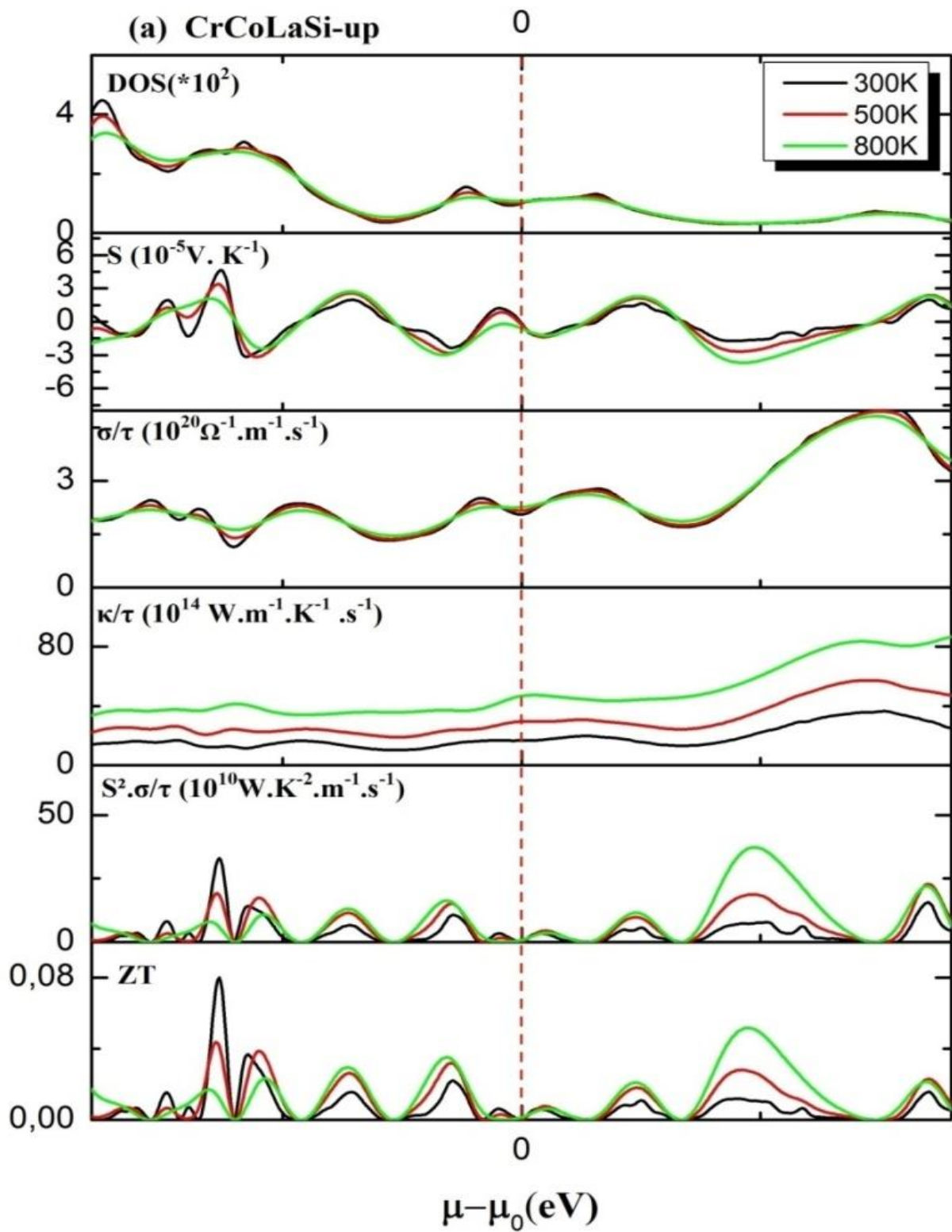


Figure 19. Density of states, Seebeck coefficient S , electrical conductivity (σ/τ), electronic thermal conductivity (κ/τ), PF and the figure of merit (ZT) for CrCoLaSi –up Heusler compound.

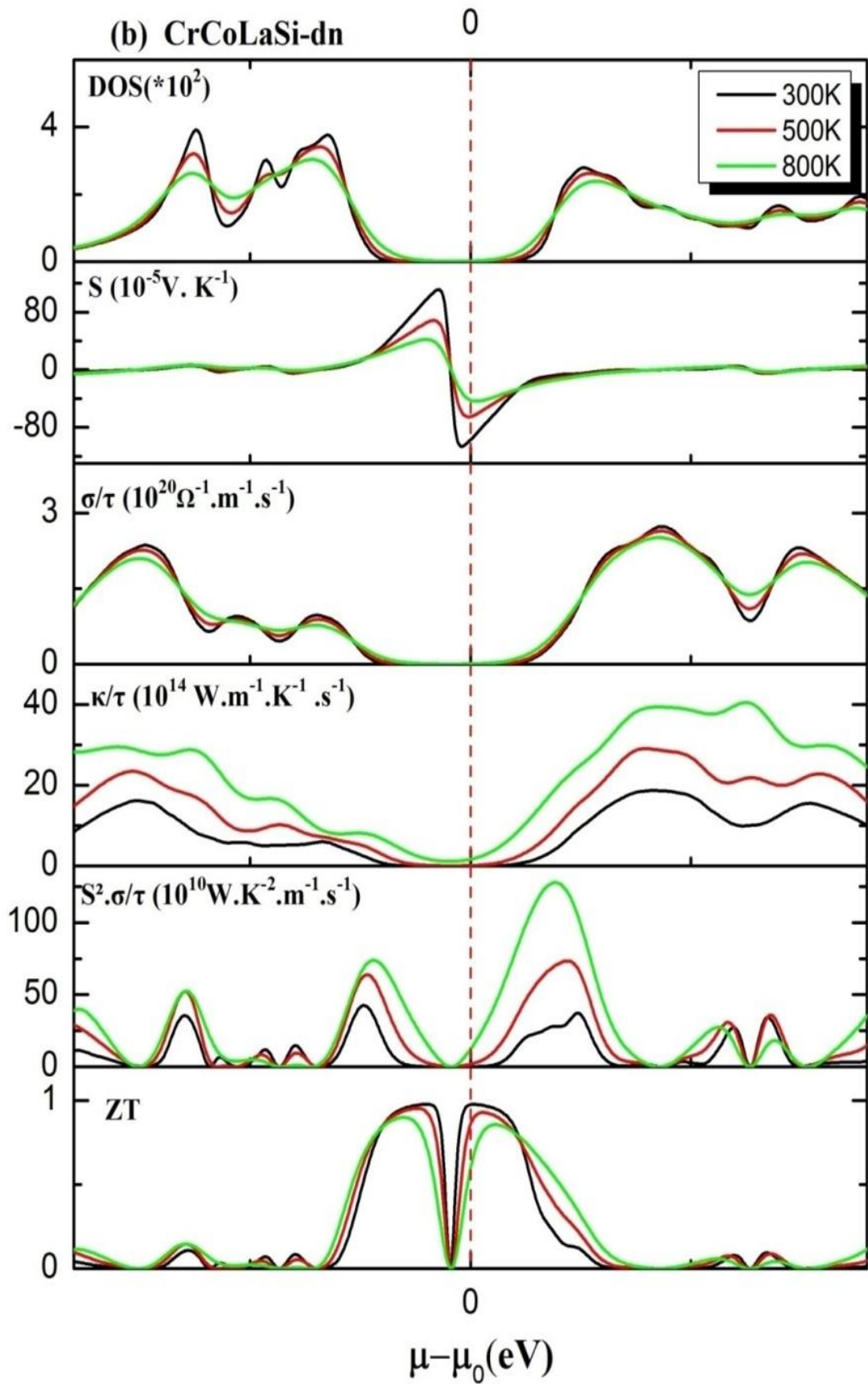


Figure 20. Density of states, Seebeck coefficient S , electrical conductivity (σ/τ), electronic thermal conductivity (κ/τ), PF and the figure of merit (ZT) for CrCoLaSi-dn Heusler compound.

Table 4 : Seebeck coefficient, the electrical resistivity, thermal conductivity and ZT when the PF takes the max value at 300 K for CrCoLaGa and CrCoLaSi compounds.

	Spin		PF $10^{10}W.m^{-1}K^{-2}s^{-1}$	S $10^{-5}V.K^{-1}$	(σ/τ) $10^{20}\Omega^{-1}.m^{-1}s^{-1}$	(κ/τ) $10^{14}W.m^{-1}K^{-1}s^{-1}$	ZT	ZT_{max}
CrCoLaGa	Spin-up	Before E_F	30.5	-4.57	1.45	10.6	0.08	0.97
		After E_F	9.92	-2.52	2.4	17.99	0.016	
	Spin-dn	Before E_F	83.73	10.84	0.71	6.80	0.36	
		After E_F	21.42	14.57	0.1	1.22	0.52	
CrCoLaSi	Spin-up	Before E_F	30.9	-5.29	1.1	9.07	0.1	0.97
		After E_F	15.61	1.96	40.0	29.93	0.015	
	Spin-dn	Before E_F	42.52	14.02	0.21	2.45	0.51	
		After E_F	37.22	5.70	1.14	9.05	0.12	

4. CONCLUSIONS

In this work, we have studied the structural, electronic, magnetic, thermodynamic, and finally thermoelectric properties of the quaternary Heusler compounds CrCoLaGa and CrCoLaSi. The study showed that both compounds are stable in the type III –ferromagnetic phase and have half-metal character. The study of chemical bonding properties had shown the existence of ionic and covalent bonds. Indeed, the ionic bond is between Cr-Cr atoms and covalent bond is between Co-Co atoms. Also, we have found that the magnetic moment of CrCoLaGa (3.21 μ B) is greater than the magnetic moment of CrCoLaSi (3.16 μ B). The thermodynamic properties are predicted by the quasi-harmonic model of Debye in the range of pressure from 0 to 20 GPa and temperature from 0 to 1200 K. This study allowed us to have a global idea on the effect of temperature and pressure on certain macroscopic parameters such as the volume V , the molar heat capacity C_v , the Debye temperature θ_D and the coefficient of thermal expansion α . The calculated thermoelectric parameters categorized our compounds as good candidates for thermoelectric applications.

Acknowledgment.

Success of this project depends largely on the encouragement, efforts, determination, and contribution of all authors.

Declarations:**Conflicts of Interest:**

The author declares no conflict of interests.

Competing interests:

The authors declare that they have no known competing financial interests or personal relationships that could have appeared to influence the work reported in this paper.

Ethical Approval:

Institutional Review Board Statement: Not applicable.

Funding:

This research work did not receive any specific grant from funding agencies in the public, commercial, or not-for-profit sectors.

Availability of data and materials:

All data is available in the article.

References :

- [1] Jourdan, M., Minár, J., Braun, J., Kronenberg, A., Chadov, S., Balke, B., ... & Kläui, M. (2014). Direct observation of half-metallicity in the Heusler compound Co_2MnSi . *Nature communications*, 5(1), 3974.
<https://doi.org/10.1038/ncomms4974>
- [2] Guan-Nan, L., Ying-Jiu, J., & Il, L. J. (2010). Effect of local atomic disorder on the half-metallicity of full-Heusler Co_2FeSi alloy: a first-principles study. *Chinese Physics B*, 19(9), 097102.
<https://iopscience.iop.org/article/10.1088/1674-1056/19/9/097102/meta>
- [3] Zhao, K., Zhang, K., Wang, J. J., Yu, J., & Wu, S. X. A first principles study on tetragonal distortion, magnetic property and elastic constants of Pd_2CrAl Heusler alloy.
<http://wulixb.iphy.ac.cn/EN/10.7498/aps.60.127101>
- [4] Cheng, Z. M., Wang, X. Q., Wang, F., Lu, L. Y., Liu, G. B., Duan, Z. F., & Nie, Z. X. First-principles study on electronic structure and half-metallic ferromagnetism of ternary compound ZnCrS .
<http://aps.cpsjournals.org.cn/EN/abstract/abstract18855.shtml>
- [5] Gao, Y. C., & Wang, X. T. (2015). First principles study on d0 half-metallic properties of full-Heusler compounds RbCaX_2 ($X = \text{C, N, and O}$). *Chinese Physics B*, 24(6), 067102.
<https://iopscience.iop.org/article/10.1088/1674-1056/24/6/067102/meta>
- [6] Liu, Z. H., Zhang, M., Cui, Y. T., Zhou, Y. Q., Wang, W. H., Wu, G. H., ... & Xiao, G. (2003). Martensitic transformation and shape memory effect in ferromagnetic Heusler alloy Ni_2FeGa . *Applied physics letters*, 82(3), 424-426.
<https://doi.org/10.1063/1.1534612>
- [7] Guermit, Y., Caid, M., Rached, D., Drief, M., Rekab-Djabri, H., Lantri, T., ... & Benkhattou, N. (2021). Investigation of structural, elastic, electronic, magnetic and thermoelectric properties for Mn_2RhZ ($Z = \text{Al, Si and Ge}$) full-Heusler alloys. *International Journal of Thermophysics*, 42, 1-18.
<https://doi.org/10.1007/s10765-021-02841-w>
- [8] Kainuma, R., Imano, Y., Ito, W., Sutou, Y., Morito, H., Okamoto, S., ... & Ishida, K. (2006). Magnetic-field-induced shape recovery by reverse phase transformation. *Nature*, 439(7079), 957-960.
<https://doi.org/10.1038/nature04493>
- [9] Tan, C. L., Tian, X. H., & Cai, W. (2008). CONDENSED MATTER: ELECTRONIC STRUCTURE, ELECTRICAL, MAGNETIC, AND OPTICAL PROPERTIES: Effect of Fe on Martensitic Transformation of NbRu High-Temperature Shape Memory Alloys: Experimental and Theoretical Study. *Chinese Physics Letters*, 25(9), 3372-3374.
<https://iopscience.iop.org/article/10.1088/0256-307X/25/9/074>
- [10] Wei, X. P., Cao, T. Y., Sun, X. W., Gao, Q., Gao, P., Gao, Z. L., & Tao, X. M. (2020). Structural, electronic, and magnetic properties of quaternary Heusler CrZrCoZ compounds: A first-principles study. *Chinese Physics B*, 29(7), 077105.
<https://iopscience.iop.org/article/10.1088/1674-1056/ab969b/meta>
- [11] Li, G. T., Liu, Z. H., Meng, F. Y., Ma, X. Q., & Wu, G. H. (2013). Effects of Cu on the martensitic transformation and magnetic properties of $\text{Mn}_{50}\text{Ni}_{40}\text{In}_{10}$ alloy. *Chinese Physics B*, 22(12), 126201.

<https://iopscience.iop.org/article/10.1088/1674-1056/22/12/126201/meta>

[12] Guermit, Y., Drief, M., Lantri, T., Tagrerout, A., Rached, H., Benkhattou, N. E., & Rached, D. (2020). Theoretical investigation of magnetic, electronic, thermoelectric and thermodynamic properties of Fe₂TaZ (Z= B, In) compounds by GGA and GGA+ U approaches. *Computational Condensed Matter*, 22, e00438.

<https://doi.org/10.1016/j.cocom.2019.e00438>.

[13] Xu, G. Z., Liu, E. K., Du, Y., Li, G. J., Liu, G. D., Wang, W. H., & Wu, G. H. (2013). EPL 102, 17007 (2013).

<https://iopscience.iop.org/article/10.1209/0295-5075/102/17007/meta>

[14] Gao, Q., Xie, H. H., Li, L., Lei, G., Deng, J. B., & Hu, X. R. (2015). First-principle study on some new spin-gapless semiconductors: The Zr-based quaternary Heusler alloys. *Superlattices and Microstructures*, 85, 536-542.

<https://doi.org/10.1016/j.spmi.2015.05.049>.

[15] Gao, Q., Opahle, I., & Zhang, H. (2019). High-throughput screening for spin-gapless semiconductors in quaternary Heusler compounds. *Physical Review Materials*, 3(2), 024410.

<https://doi.org/10.1103/PhysRevMaterials.3.024410>

[16] Khan, M., Dubenko, I., Stadler, S., & Ali, N. (2007). Exchange bias behavior in Ni–Mn–Sb heusler alloys. *Applied Physics Letters*, 91(7).

<https://doi.org/10.1063/1.2710779>

[17] Liu, J., Gottschall, T., Skokov, K. P., Moore, J. D., & Gutfleisch, O. (2012). Giant magnetocaloric effect driven by structural transitions. *Nature materials*, 11(7), 620-626.

<https://doi.org/10.1038/nmat3334>

[18] Zhang, X. (2018). Theoretical design of multifunctional half-Heusler materials based on first-principles calculations. *Chinese Physics B*, 27(12), 127101.

<https://iopscience.iop.org/article/10.1088/1674-1056/27/12/127101/meta>

[19] Wei, X. P., Gao, P., & Zhang, Y. L. (2020). Investigations on Gilbert damping, Curie temperatures and thermoelectric properties in CoFeCrZ quaternary Heusler alloys. *Current Applied Physics*, 20(4), 593-603.

<https://doi.org/10.1016/j.cap.2020.02.007>.

[20] Wernick, J. H., Hull, G. W., Geballe, T. H., Bernardini, J. E., & Waszczak, J. V. (1983). Superconductivity in ternary Heusler intermetallic compounds. *Materials Letters*, 2(2), 90-92.

[https://doi.org/10.1016/0167-577X\(83\)90043-5](https://doi.org/10.1016/0167-577X(83)90043-5).

[21] Wolf, S. A., Awschalom, D. D., Buhrman, R. A., Daughton, J. M., von Molnár, V. S., Roukes, M. L., ... & Treger, D. M. (2001). Spintronics: a spin-based electronics vision for the future. *science*, 294(5546), 1488-1495. <https://www.science.org/doi/10.1126/science.1065389>.

[22] Graf, T., Felser, C., & Parkin, S. S. (2011). Simple rules for the understanding of Heusler compounds. *Progress in solid state chemistry*, 39(1), 1-50.

<https://doi.org/10.1016/j.progsolidstchem.2011.02.001>.

[23] Tavares, S., Yang, K., & Meyers, M. A. (2023). Heusler alloys: Past, properties, new alloys, and prospects. *Progress in Materials Science*, 132, 101017.

<https://doi.org/10.1016/j.pmatsci.2022.101017>.

[24] Guermit, Y., Drief, M., Benkhattou, N. E., Lantri, T., Abidri, B., & Rached, D. (2018). Phase stability, electronic, magnetic and elastic properties of Ni₂CoZ (Z= Ga, Sn): A first principles study with GGA method and GGA+ U approach. *Chinese Journal of Physics*, 56(4), 1394-1404.

<https://doi.org/10.1016/j.cjph.2018.05.015>.

[25] Drews, J., Eberz, U., & Schuster, H. U. (1986). Optische Untersuchungen an farbigen Intermetallischen Phasen. *Journal of the Less Common Metals*, 116(1), 271-278.

[https://doi.org/10.1016/0022-5088\(86\)90235-3](https://doi.org/10.1016/0022-5088(86)90235-3).

[26] Dai, X., Liu, G., Fecher, G. H., Felser, C., Li, Y., & Liu, H. (2009). New quaternary half metallic material CoFeMnSi. *Journal of Applied Physics*, 105(7).

<https://doi.org/10.1063/1.3062812>

[27] Liu, J. R., Wei, X. P., Chang, W. L., & Tao, X. (2022). Structural stability, electronic, magnetic and thermoelectric properties for half-metallic quaternary Heusler alloys CrLaCoZ. *Journal of Physics and Chemistry of Solids*, 163, 110600.

<https://doi.org/10.1016/j.jpcs.2022.110600>.

[28] Priyanka, D. S., Sudharsan, J. B., Srinivasan, M., & Ramasamy, P. (2022). Cobalt based new quaternary Heusler alloys for Spintronic and thermoelectric applications: an Ab-initio study. *Materials Technology*, 37(11), 1936-1946.

<https://doi.org/10.1080/10667857.2021.2014030>

[29] Shakil, M., Arshad, H., Zafar, M., Rizwan, M., Gillani, S. S. A., & Ahmed, S. (2020). First-principles computation of new series of quaternary Heusler alloys CoScCrZ (Z= Al, Ga, Ge, In): a study of structural, magnetic, elastic and thermal response for spintronic devices. *Molecular Physics*, 118(24), e1789770.

<https://doi.org/10.1080/00268976.2020.1789770>

[30] Shakil, M., Sadia, H., Gillani, S. S. A., Shahid, M., Rizwan, M., Gadhi, M. A., ... & Alrobei, H. (2021). Computation of structural, mechanical, thermal, and magnetic characteristics of newly designed Quaternary Heusler alloys CoNbCrZ (Z= Al, Ga, Si, Ge). *Journal of Superconductivity and Novel Magnetism*, 34, 3243-3254.

<https://doi.org/10.1007/s10948-021-06066-8>

[31] Li, Y., Liu, G. D., Wang, X. T., Liu, E. K., Xi, X. K., Wang, W. H., ... & Dai, X. F. (2017). First-principles study on electronic structure, magnetism and half-metallicity of the NbCoCrAl and NbRhCrAl compounds. *Results in physics*, 7, 2248-2254.

<https://doi.org/10.1016/j.rinp.2017.06.047>

[32] Blaha, P., Schwarz, K., Madsen, G. K., Kvasnicka, D., & Luitz, J. (2001). wien2k. *An augmented plane wave+ local orbitals program for calculating crystal properties*, 60(1).

<https://www.scholars.northwestern.edu/en/publications/wien2k-an-augmented-plane-wave-plus-local-orbitals-program-for-ca>

- [33] Blaha, P., Schwarz, K., Sorantin, P., & Trickey, S. B. (1990). Full-potential, linearized augmented plane wave programs for crystalline systems. *Computer physics communications*, 59(2), 399-415.
[https://doi.org/10.1016/0010-4655\(90\)90187-6](https://doi.org/10.1016/0010-4655(90)90187-6)
- [34] Schwarz, K., Blaha, P., & Madsen, G. K. (2002). Electronic structure calculations of solids using the WIEN2k package for material sciences. *Computer physics communications*, 147(1-2), 71-76.
[https://doi.org/10.1016/S0010-4655\(02\)00206-0](https://doi.org/10.1016/S0010-4655(02)00206-0)
- [35] Perdew, J. P., Burke, K., & Ernzerhof, M. (1996). Generalized gradient approximation made simple. *Physical review letters*, 77(18), 3865.
<https://doi.org/10.1103/PhysRevLett.77.3865>
- [36] Perdew, J. P., Burke, K., & Wang, Y. (1996). Generalized gradient approximation for the exchange-correlation hole of a many-electron system. *Physical review B*, 54(23), 16533.
<https://doi.org/10.1103/PhysRevB.54.16533>
- [37] Blanco, M. A., Pendás, A. M., Francisco, E., Recio, J. M., & Franco, R. (1996). Thermodynamical properties of solids from microscopic theory: applications to MgF₂ and Al₂O₃. *Journal of Molecular Structure: THEOCHEM*, 368, 245-255.
[https://doi.org/10.1016/S0166-1280\(96\)90571-0](https://doi.org/10.1016/S0166-1280(96)90571-0)
- [38] Flórez, M., Recio, J. M., Francisco, E., Blanco, M. A., & Pendás, A. M. (2002). First-principles study of the rocksalt–cesium chloride relative phase stability in alkali halides. *Physical Review B*, 66(14), 144112.
<https://doi.org/10.1103/PhysRevB.66.144112>
- [39] Francisco, E., Recio, J. M., Blanco, M. A., Pendás, A. M., & Costales, A. (1998). Quantum-mechanical study of thermodynamic and bonding properties of MgF₂. *The Journal of Physical Chemistry A*, 102(9), 1595-1601.
<https://pubs.acs.org/doi/10.1021/jp972516j>
- [40] Blanco, M. A., Francisco, E., & Luana, V. (2004). GIBBS: isothermal-isobaric thermodynamics of solids from energy curves using a quasi-harmonic Debye model. *Computer Physics Communications*, 158(1), 57-72.
<https://doi.org/10.1016/j.comphy.2003.12.001>
- [41] Alijani, V., Winterlik, J., Fecher, G. H., Naghavi, S. S., & Felser, C. (2011). Quaternary half-metallic Heusler ferromagnets for spintronics applications. *Physical Review B*, 83(18), 184428.
<https://doi.org/10.1103/PhysRevB.83.184428>
- [42] Murnaghan, F. D. (1944). The compressibility of media under extreme pressures. *Proceedings of the National Academy of Sciences*, 30(9), 244-247.
<https://doi.org/10.1073/pnas.30.9.244>
- [43] Liu, J. R., Wei, X. P., Chang, W. L., & Tao, X. (2022). Structural stability, electronic, magnetic and thermoelectric properties for half-metallic quaternary Heusler alloys CrLaCoZ. *Journal of Physics and Chemistry of Solids*, 163, 110600.
<https://doi.org/10.1016/j.jpcs.2022.110600>
- [44] Dulong, P. L., & Petit, A. T. (1819). *Recherches sur quelques points importants de la theorie de la chaleur*, Annales de Chimie et de Physique, Vol. 10, pp. 395-413.

http://www.ffn.ub.es/luisnavarro/nuevo_maletin/Petit--Dulong_1819.pdf

[45] Xia, Y. Q., Gao, Y. L., Yan, L. P., & Fu, M. Y. (2015). Recent progress in networked control systems—A survey. *International Journal of Automation and Computing*, 12(4), 343-367.

<https://doi.org/10.1007/s11633-015-0894-x>

[46] Madsen, G. K., & Singh, D. J. (2006). BoltzTraP. A code for calculating band-structure dependent quantities. *Computer Physics Communications*, 175(1), 67-71.

<https://doi.org/10.1016/j.cpc.2006.03.007>

[47] He, J., Amsler, M., Xia, Y., Naghavi, S. S., Hegde, V. I., Hao, S., ... & Wolverton, C. (2016). Ultralow thermal conductivity in full Heusler semiconductors. *Physical review letters*, 117(4), 046602.

<https://doi.org/10.1103/PhysRevLett.117.046602>

[48] Rabina, O., Lin, Y. M., & Dresselhaus, M. S. (2001). Anomalously high thermoelectric figure of merit in Bi_{1-x}Sb_x nanowires by carrier pocket alignment. *Applied Physics Letters*, 79(1), 81-83.

<https://doi.org/10.1063/1.1379365>

[49] Takeuchi, T. (2009). Conditions of electronic structure to obtain large dimensionless figure of merit for developing practical thermoelectric materials. *Materials transactions*, 50(10), 2359-2365.

<https://doi.org/10.2320/matertrans.M2009143>